



A Hybrid Deep-Learning and Evolutionary Feature-Selection Framework for Skin Lesion Classification: Application to Monkeypox Detection

Nidhi Chauhan, Alok Singh Chauhan*

School of Computing Science and Engineering, Galgotias University, Greater Noida 203201, India

***alok.chauhan@galgotiasuniversity.edu.in**

Abstract. The recent resurgence of Monkeypox has highlighted the urgent need for fast and accurate diagnostic tools. In this paper, we propose a new framework of hybrid deep learning to combine both DenseNet121 and MobileNetV2 to obtain both rich and supplementary attributes of the skin lesion images. By pooling the outputs of these two models in terms of features, we get the lightweight representation of the images as well as rich representations of the images. To improve the feature set, we use Genetic Algorithm (GA) which is useful in reducing the dimensions and eliminating redundancy. Optimized features are then categorized with the help of the Random Forest model, which has been selected due to its good performance and capacity to work with high-dimensional data. Using two publicly accessible datasets, MSID and MSLD, we tested our approach and obtained remarkable classification accuracies of 92.71% and 97.77%, respectively. These findings highlight the success of combining ensemble learning, evolutionary optimization, and deep learning to achieve accuracy and proper diagnosis of monkeypox through medical images.

Keywords: Monkeypox Detection, Deep Learning, Genetic Algorithm, Feature Selection, Random Forest, Hybrid Neural Network, Image classification, Medical imaging

(Received 2025-09-20, Revised 2025-12-17, Accepted 2025-12-22, Available Online by 2026-01-21)

1. Introduction

Monkeypox is a re-emerging zoonotic disease that presents with dermatological symptoms, most notably skin lesions that can closely resemble those of other skin diseases like chickenpox and measles. Fast and proper diagnosis is a major tool in the control of outbreaks and the provision of effective timely treatment particularly in resource-constrained environments where laboratory tests like PCR might be inaccessible. Consequently, there is an increasing research interest in the development of the automated and image-based diagnostic tools. The use of deep learning (DL) specifically convolutional neural networks (CNNs) has shown great promise in the analysis of medical images [[1]-[2]]. Deep neural networks such as DenseNet121 and MobileNetV2 are commonly used due to their good performance

feature extraction with a compromise in depth and computation efficiency. Nonetheless, using one CNN may limit the variety of characteristics that could be learnt using complex medical images. It is possible to combine several CNN designs to enhance the feature richness and better diagnostics. One of the primary challenges of such systems is the large dimensionality of deep features that often have redundant or unnecessary information. This can have an adverse effect on model generalization. To overcome this, one can use Genetic Algorithms (GAs) that imitate natural selection to be able to find the most informative subset of features, as it is very effective at searching for very large and complex feature spaces. Specifically, ensemble methods like Random Forests are well-suited to process various and high-dimensional data to classify it and offer trustworthy and understandable predictions. This paper introduces a combined model that consists of feature extraction with two CNN models (DenseNet121 and MobileNetV2), feature selection with a Genetic Algorithm, and the final classification with a Random Forest. This model is applicable to clinical practice and remote healthcare because it aims at the high accuracy of a diagnosis and lower computational load. Two publicly available datasets of skin lesion images are used to determine the effectiveness of the proposed framework. Stricter validation is maintained with greater caution such as relevant data partitioning and assessment methods to avoid overfitting. Key contributions of this work include:

- A novel hybrid pipeline combining dual CNN architectures, evolutionary feature selection, and ensemble classification.
- Effective fusion of deep features from DenseNet121 and MobileNetV2.
- Dimensionality reduction based on GA to improve classification performance.
- Integration with a Random Forest classifier to increase robustness and interpretability.
- Extensive empirical validation showing notable advancements over baseline models.

Previous studies have explored various deep learning architectures for Monkeypox detection. The study by [[3]] introduced DeepGenMon, integrating attention-based CNNs with Genetic Algorithms to optimize hyperparameters, resulting in improved classification performance. [[4]] utilized MobileNetV2 for feature extraction, achieving high accuracy in distinguishing Monkeypox from other skin conditions. The advancement of computer-aided diagnostic (CAD) systems has significantly transformed dermatological disease detection, especially with the integration of artificial intelligence (AI). In recent years, convolutional neural networks (CNNs) and transfer learning models have proven effective in classifying complex dermoscopic images with high accuracy [[5]][[27]]. Transfer learning frameworks such as VGG16, VGG19, ResNet-50, DenseNet121, InceptionV3, and MobileNetV2 have been leveraged to compensate for the limited availability of annotated medical image datasets, demonstrating notable performance in multi-class skin lesion classification tasks [[6]]. Recent research has increasingly explored hybrid approaches that combine the strengths of both deep learning (DL) and machine learning (ML) for detecting monkeypox from skin lesion images. Eliwa, et.al uses GWO optimization method to optimize CNNs, which are well-known for their efficacy in image classification tasks. Accuracy, precision, recall, F1-score, and AUC are just a few of the performance measures that significantly increase when the CNN hyperparameters are adjusted with the aid of the GWO. [[7]]. Similarly, [[7]] utilized a hybrid deep learning model for the classification of skin diseases—including monkeypox—within the Internet of Medical Things (IoMT) context, effectively merging CNN-based feature extraction with traditional ML classifiers like SVM and Random Forest to optimize real-time deployment performance. [[9]] combined Vision Transformers with classic augmentation techniques and transfer learning models such as InceptionV3 to improve robustness against small sample sizes in monkeypox classification.

Another notable effort by [[10]] introduced a federated learning-enhanced model using pre-trained CNNs to detect monkeypox lesions efficiently while preserving patient data privacy across decentralized nodes. A broader synthesis by [[11]] also reviewed various hybrid frameworks that combine DL models like CNNs and Transformers with ML classifiers to improve generalizability and reduce overfitting in monkeypox lesion identification. [[12]] emphasized the value of hybrid texture and statistical feature

extraction combined with DL classifiers, resulting in enhanced multiclass discrimination between monkeypox, chickenpox, and other diseases.

Recent advancements in artificial intelligence have spurred the development of hybrid systems combining deep learning (DL), machine learning (ML), and genetic algorithms (GA) for the early detection of monkeypox through skin lesion images. One of the most notable efforts is [[13]][[24]] that developed a diagnostic pipeline using binary genetic algorithms (GA) and binary firefly optimization to refine feature selection in DL models trained on monkeypox lesions. [[14]] extended this by employing ANN+GA ensembles in an IoT-integrated DL system, emphasizing its potential for mobile-based screening tools. Furthermore, [[15]] applied a GA-based feature selection method to optimize DL models and demonstrated improved performance in multiclass skin lesion classification, including monkeypox. [[16]] combined high-performing CNNs with a GA-driven feature reduction strategy to develop a hybrid DL model for monkeypox, validating it across a noisy, unbalanced dataset with superior precision and recall metrics. These hybrid systems illustrate a growing consensus: combining DL's representation power with ML's interpretability and GA's optimization can yield robust, scalable models suitable for both clinical and remote diagnostic settings.

However, limited research has combined multiple deep learning models with machine learning classifiers and optimization techniques in a unified framework for Monkeypox detection. This study aims to fill this gap by integrating MobileNetV2, DenseNet121, Random Forest, and Genetic Algorithm optimization

2. Methods

The suggested hybrid diagnostic system, which combines a Random Forest (RF) classifier for monkeypox diagnosis, a Genetic Algorithm (GA) for feature selection, and deep learning for feature extraction, is described in this section. Dataset preparation, preprocessing, dual CNN-based feature extraction, GA-based feature selection, Random Forest classification, and performance evaluation are the six main parts of the procedure. This hybrid approach for detecting Monkeypox is visualized in **Error! Reference source not found.**

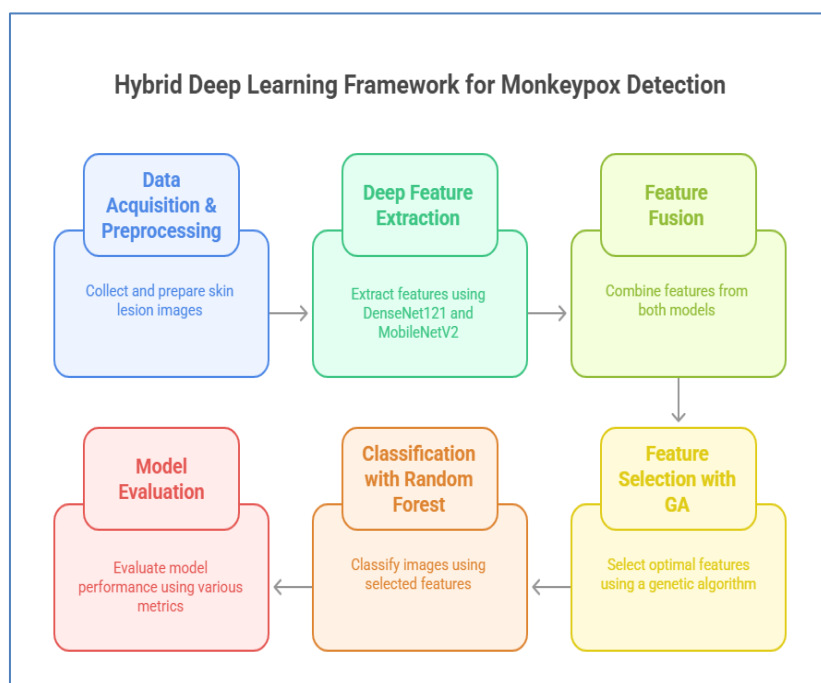


Figure 1. Hybrid framework used in the study

2.1. Dataset

The study utilizes a publicly available Monkeypox skin lesion dataset comprising images labelled as Monkeypox and normal skin conditions [[23]]. The dataset includes diverse skin tones and lesion presentations to ensure model generalizability. The datasets are already pre-processed including image normalization, resizing, and augmentation to enhance model generalization.

Monkeypox Skin Image Dataset (MSID) – 477 images categorized into Monkeypox, chickenpox, and measles classes which are collectively placed into Normal class.

Monkeypox Skin Lesion Detection (MSLD) – 2,607 images classified as Monkeypox or normal skin conditions. Dataset distribution for each dataset is shown in Table 1. All the datasets being used perform binary classification.

Table 1. Dataset distribution

Dataset	Label	Train	Validation	Test	Total
MSID	Monkeypox	223	56	0	279
	Normal (Chickenpox + Measles)	158	40	0	198
	Total	381	96	0	477
MSLD	Monkeypox	980	20	168	1168
	Normal	1162	25	252	1439
	Total	2142	45	420	2607

Some sample images of Monkeypox disease from both the datasets are shown in **Error! Reference source not found..**



Figure 2. Sample images of Monkeypox disease from the two datasets used in this study.

2.2. Feature Extraction using Deep Learning Models(MobileNetV2+DenseNet121)

This study uses a dual-model strategy employing DenseNet121 and MobileNetV2 for feature extraction to take advantage of multiple convolutional neural networks (CNNs). These models were selected due to their complementary characteristics. While MobileNetV2 is designed for efficiency and lightweight deployment, especially for edge and mobile applications, DenseNet121 enables dense connectivity with rich feature hierarchies.

Model Selection and Fine-tuning:

Both models were pretrained on ImageNet and subsequently fine-tuned on the Monkeypox skin lesion datasets. The classification layers were removed, and Global Average Pooling (GAP) was applied to extract fixed-length feature vectors from each architecture. [[17]]

Feature Fusion Strategy:

A complete and high-dimensional feature representation was created by concatenating features taken from both models. Different levels of abstraction are captured by this fusion strategy: MobileNetV2

adds lightweight and spatially efficient features, while DenseNet121 contributes rich semantic representations.

Let each input image be denoted as $x \in \mathbb{R}^{224 \times 224 \times 3}$. DenseNet121 and MobileNetV2 extract hierarchical features from images. Mathematically, these can be represented as (1) and (2)

$$f_D(x): \mathbb{R}^{224 \times 224 \times 3} \rightarrow \mathbb{R}^{d1} \quad (1)$$

$$f_M(x): \mathbb{R}^{224 \times 224 \times 3} \rightarrow \mathbb{R}^{d2} \quad (2)$$

where d_1 and d_2 are the dimensions of the feature vectors extracted by DenseNet121 and MobileNetV2, respectively. The combined feature vector for an image x is represented as (3)

$$F(x) = [f_D(x); f_M(x)] \in \mathbb{R}^d, \text{ where } d = d_1 + d_2 \quad (3)$$

2.3. Feature Selection using Genetic Algorithm

CNN-generated high-dimensional feature vectors frequently have non-discriminative, redundant, or irrelevant components that could negatively impact classification performance [18]. In order to address this problem, feature selection is carried out using a Genetic Algorithm (GA), which optimizes the subset of features for downstream classification.

Genetic Algorithm Overview:

Natural selection and genetic inheritance serve as the foundation for the GA, an evolutionary optimization method. It finds the ideal subset of attributes that maximizes classification accuracy by evolving a population of possible solutions (chromosomes) over several generations.

Each chromosome is encoded as a binary vector $z \in \{0,1\}^d$, where:

- $z_i=1$ indicates the inclusion of the i^{th} feature.
- $z_i=0$ indicates exclusion of the i^{th} feature.

The selected features for an image x based on a chromosome z are denoted as $F_z(x) \subseteq F(x)$ [[19], [25]].

Fitness Evaluation:

The fitness of each chromosome is evaluated using the classification accuracy of a Random Forest (RF) classifier trained on the selected features. Five-fold cross-validation is used for reliable fitness estimation [[20]]. The fitness function is defined as:

$$\text{Fitness}(z) = \text{Accuracy} \text{ (Classifier trained on } F_z(x) \text{)} \quad (4)$$

The GA iteratively evolves the population to maximize the fitness function, resulting in an optimal feature subset $F_{\text{opt}}(x)$. Our initial tests showed diminishing benefits beyond moderate population sizes when combined with Optuna tuning and cross-validation, even though standard GAs employ enormous populations. A sensitivity study was performed to evaluate population sizes $\in \{10, 20, 40, 60\}$ and generations $\in \{5, 10, 20\}$. Each configuration was tested on the MSID dataset using 5-fold cross-validation. Therefore, population = 20 and generations = 10 were selected as a balanced trade-off between performance and computational cost [[28]]. This decision was reinforced by Optuna's trial-based optimization, which confirmed near-plateau fitness improvements beyond these values. Hyperparameters tuned for GA+Random Forest is shown in Table 2. When compared to manually specified parameters, the optimized configuration consistently produced lower overfitting and higher validation accuracy. Both the evolutionary and ensemble learning components were optimized in a repeatable, data-driven manner due to this adaptive search technique.

Table 2. Hyperparameter tuning of GA+Random Forest parameters

GA parameters	Random Forest parameters
---------------	--------------------------

Population size $\in \{10, 20, 30, 40\}$	Number of trees ($n_estimators$) $\in \{100, 200, 300, 400, 500\}$
Crossover probability $\in [0.3, 0.8]$	Maximum depth (max_depth) $\in \{\text{None}, 10 - 50\}$
Mutation probability $\in [0.05, 0.3]$	Minimum samples per leaf ($min_samples_leaf$) $\in \{1, 2, 4\}$
Number of generations $\in \{5 - 20\}$	Criterion $\in \{\text{"gini"}, \text{"entropy"}\}$
Feature subset ratio $\in [0.2, 0.8]$	Bootstrap $\in \{\text{True}, \text{False}\}$

2.4. Classification with Machine Learning Classifier

A Random Forest (RF) classifier was used in this study rather than an end-to-end fine-tuned CNN classifier for several reasons beyond interpretability. First, heterogeneous, and high-dimensional feature spaces, as those created by combining feature maps from several CNN architectures, are a good fit for RFs. Unlike end-to-end fine-tuning, which requires large labeled datasets to optimize millions of parameters, RFs can effectively learn decision boundaries from limited data without overfitting. Second, RFs provide inherent resistance to noisy or redundant features, which is crucial even after Genetic Algorithm (GA) based selection. By combining multiple decision trees, their ensemble structure automatically reduces variation and stabilizes predictions across datasets and folds. Third, modular experimentation is made possible by separating deep feature extraction from classification using a separate RF stage. This adaptability promotes repeatability and useful deployment on constrained hardware by enabling the same optimized features to be assessed with different traditional classifiers (e.g., SVM, XGBoost) without retraining the deep network. Lastly, RFs are more suitable for integration into portable or edge-based diagnostic systems as they require less processing power and training time than fine-tuned CNNs, particularly in low-resource healthcare settings where monkeypox detection is crucial. Therefore, following feature selection, the optimal subset of features $F_{opt}(x)$ is used to train a Random Forest (RF) classifier for the final prediction task. Random Forest is an ensemble learning method composed of multiple decision trees, each trained on a bootstrapped subset of the data with random feature sampling at each node split [[21]].

Prediction Mechanism:

Let the ensemble consist of M decision trees $\{T_1, T_2, \dots, T_M\}$. Each tree provides an individual class prediction y_m for a given input sample x . The final class label \hat{y} is determined by majority voting across all trees as in (5):

$$\hat{y} = \text{mode}\{y_1, y_2, \dots, y_M\} \quad (5)$$

The following algorithm describes the entire diagnostic pipeline for classifying monkeypox utilizing Random Forest classification, Genetic Algorithm-based feature selection, and dual deep learning models.

Algorithm: Hybrid framework

Input: Skin image dataset $D = (x_i, y_i)$ where $x_i \in \mathbb{R}^{224 \times 224 \times 3}$, Labels $y_i \in \{0, 1\}$ (Monkeypox or Normal)

Output: Predicted label \hat{y} for each test image.

Begin

Step 1: Data Preprocessing

1. Resize all images to 224×224
2. Normalize pixel values to $[0, 1]$ or per model's requirements.
3. Applied 5-fold cross validation on both datasets.

Step 2: Deep Feature Extraction

3. Load pretrained **DenseNet121** and **MobileNetV2** (excluding classification head).
4. For each image $x_i \in D$
 - o Extract feature vector $f_d \leftarrow \text{DenseNet121}(x_i)$
 - o Extract feature vector $f_m \leftarrow \text{MobileNetV2}(x_i)$
 - o Concatenate: $F_i = [f_d; f_m]$

Step 3: Genetic Algorithm-Based Feature Selection

5. Initialize population of binary chromosomes representing selected features from F_i .
6. For each generation:
 - o For each chromosome:
 - Select subset of features F_i' based on the chromosome.
 - Train a Random Forest on F' using cross-validation.
 - Compute accuracy as fitness score.
 - o Apply genetic operators: selection, crossover, mutation.
7. Select best-performing chromosome → final selected feature indices.

Step 4: Classification using Random Forest

8. Train Random Forest classifier on GA-selected features.
9. Predict labels \hat{y} on test set using selected features.

Step 5: Evaluation

10. Compute metrics: Accuracy, Precision, Recall, F1-score, ROC-AUC.

Step 6: Visualization

11. Apply PCA on selected features for 2D visualization.

End

3. Results and Discussion

This section presents the performance evaluation of the proposed hybrid framework integrating DenseNet121 and MobileNetV2 for deep feature extraction, Genetic Algorithm (GA) for feature selection, and Random Forest (RF) for classification. The framework was tested on two publicly available datasets: MSID and MSLD and evaluated using accuracy, precision, recall, F1-score, ROC-AUC, and visual diagnostics. All experiments were implemented in Python using the Scikit-learn and Keras libraries.

3.1. Performance Metrics

Table 3 and

Table 4 summarize the classification results on the MSID and MSLD datasets, respectively. Each configuration incrementally incorporates the components of the proposed framework, demonstrating the additive value of ensemble learning and GA-based feature selection.

For the MSID and MSLD the base dual-CNN model (DenseNet121 + MobileNetV2) achieved 83.33% and 88.89% accuracy respectively. Incorporating a Random Forest classifier improved accuracy to 89.58% for MSID and 97.77% for MSLD. Applying Genetic Algorithm-based feature selection further boosted accuracy to 92.71% for MSID. However, 97.77% accuracy for MSLD remains same due to small dataset.

Table 3. Evaluation metrics values on MSID dataset.

Model	Accuracy	Precision	Recall	F1-Score
DenseNet121+MobileNetV2	83.33%	0.83	0.75	0.78
DenseNet121+MobileNetV2+RandomForest	89.58%	0.91	0.91	0.91
DenseNet121+MobileNetV2+RandomForest+GA	92.71%	0.90	0.92	0.91

Table 4. Evaluation metrics values on MSLD dataset.

Model	Accuracy	Precision	Recall	F1-Score
DenseNet121+MobileNetV2	88.89%	1.00	0.80	0.889
DenseNet121+MobileNetV2+RandomForest	97.77%	0.95	1.00	0.98
DenseNet121+MobileNetV2+RandomForest+GA	97.77%	1	0.96	0.98

The classification accuracy bar graph representation accuracies across different model variants are shown in **Error! Reference source not found..**

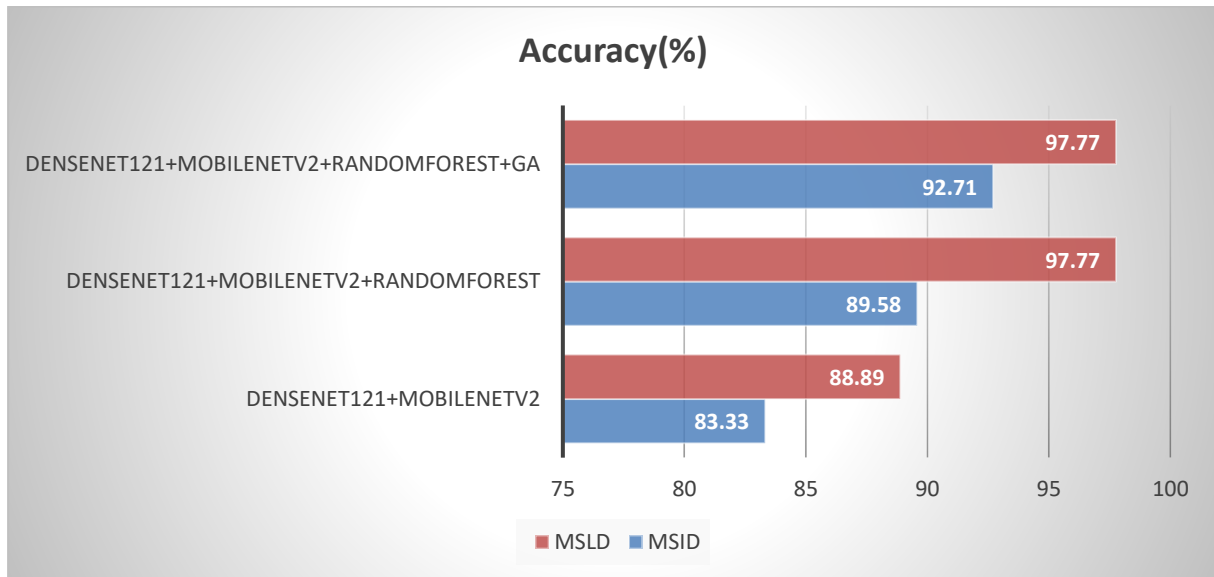


Figure 3. Bar graph representation of accuracy improvements

3.2. Feature Importance Analysis

To increase the interpretability of the proposed hybrid framework, feature importance plots have been obtained with the help of the trained Random Forest classifier. These plots measure the contribution of each of the selected features to the final decision in classification. Figure describes the feature importance scores of the data of MSID. The importance index 27 was the highest (≈ 0.032), which states that it was the most effective in separating Monkeypox and normal skin conditions. Other noteworthy features were the ones in index 493, 18, and 110 that also had high relevance scores. Likewise, Figure also shows feature importance on the MSLD dataset: Feature index 128 had the greatest importance ($= 0.032$), meaning that it was the most significant in the differentiation between Monkeypox and normal skin conditions [[26]]. The rest of the important auto features were 10, 240, and 239 which also had high relevancy scores.

The overall trend showed a gradual decline in importance from left to right, indicating a strong rank-order of discriminative power among the selected features. Feature distribution across importance values showed a compact, high-contribution core set, suggesting the optimized features are both informative and compact. Domain experts can verify whether the model's reasoning is consistent with recognized dermatological markers (such as lesion texture or edge sharpness) by selecting the most significant aspects. The analysis supports the dimensionality reduction attained by GA by confirming that a small selection of features contributes most to predictive accuracy.

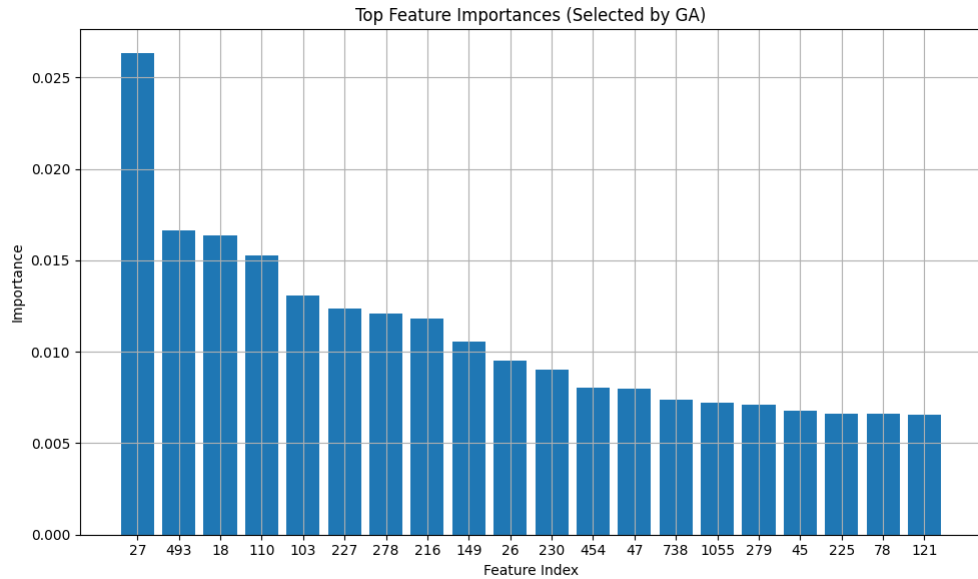


Figure 4. Bar plot of feature importances for the MSID dataset after GA optimization.

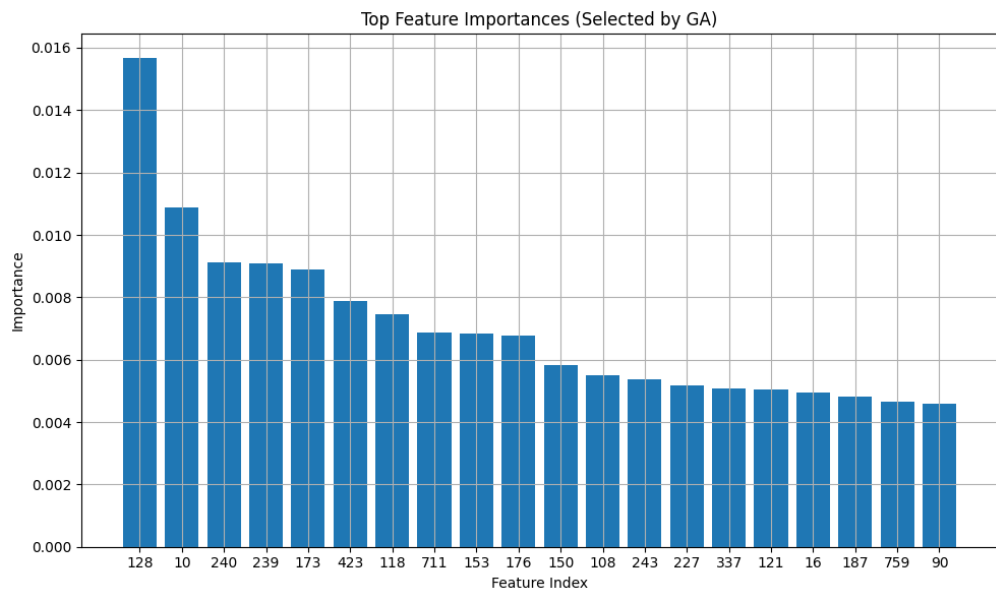


Figure 5. Bar plot of feature importance for the MSLD dataset after GA optimization.

3.3. GA Optimization Dynamics

We monitored the evolution of classification accuracy over multiple generations to assess the effectiveness of the Genetic Algorithm (GA) in choosing ideal feature subsets. The effectiveness of GA's convergence toward a high-performing solution is confirmed by this analysis. Figure and Figure depict the progression of fitness values, defined as classification accuracy, over 10 generations for the MSID and MSLD datasets, respectively. The algorithm's ability to enhance classification performance over time was confirmed by a steady rising trend in both average and maximum fitness values. As more discriminative feature subsets emerged in subsequent generations, the maximum accuracy improved progressively. The population may have evolved toward a globally optimal or nearly optimal solution if the difference between minimum and maximum accuracies is getting smaller.

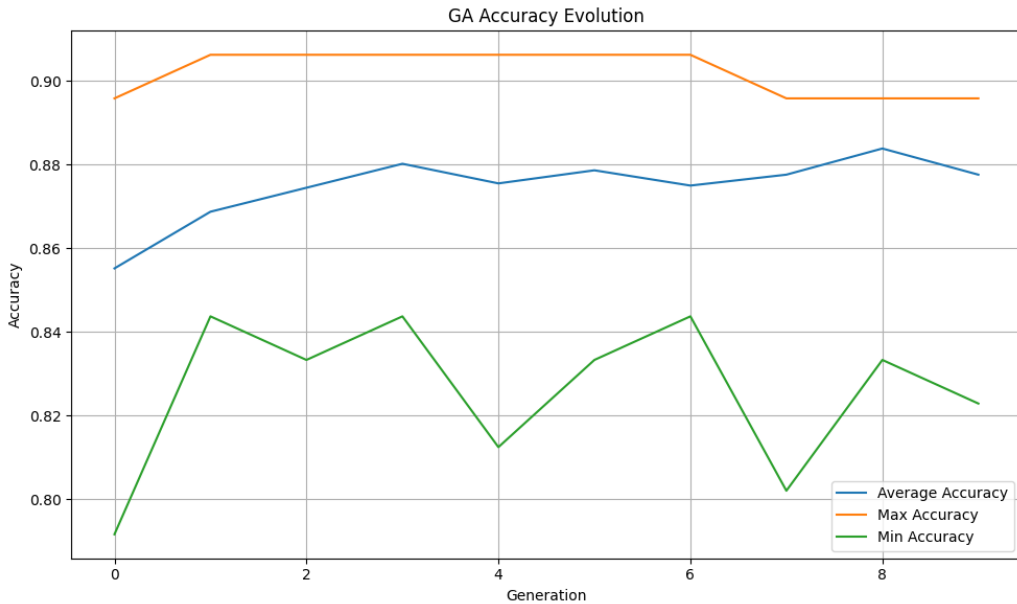


Figure 6. GA accuracy evolution across generations on the MSID dataset.

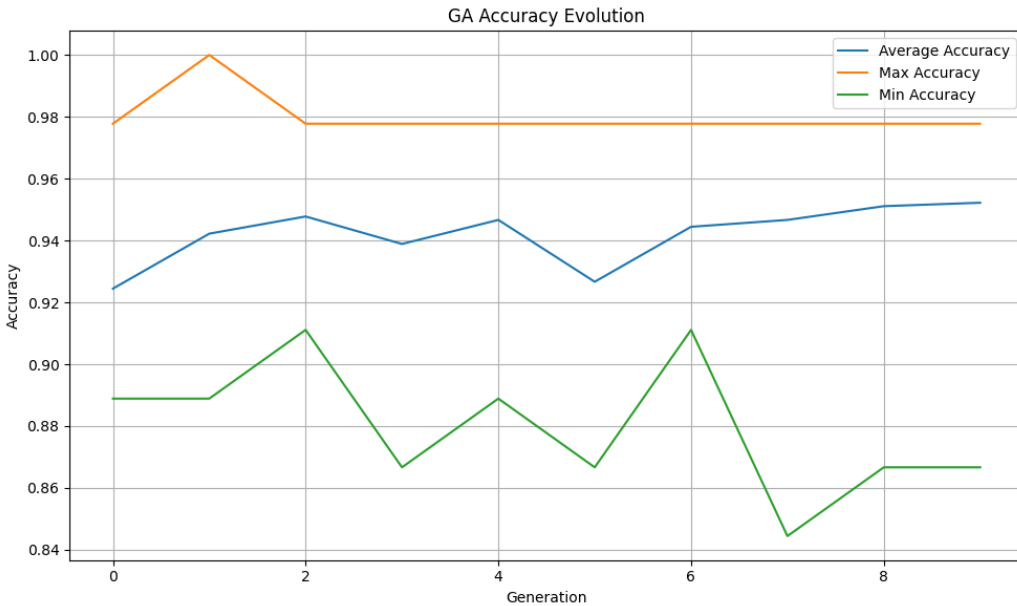


Figure 7. GA accuracy evolution across generations on the MSLD dataset.

3.4. Visual Feature Separation

To qualitatively assess the discriminative capacity of the features selected by the Genetic Algorithm, we employed widely used dimensionality reduction technique i.e. Principal Component Analysis (PCA). This visualization helps illustrate whether the selected feature space facilitates clear separation between Monkeypox and Normal classes. Figure presents 2D PCA projections of the selected features from both the MSID and MSLD datasets. Blue points represent the Normal class, while orange points correspond to Monkeypox cases. PCA reveals a reasonable degree of class separation, suggesting that the most informative directions in the feature space (principal components) capture sufficient discriminatory variance. Although PCA preserves global variance structure, some class overlap is visible, this is expected given its linear transformation nature.

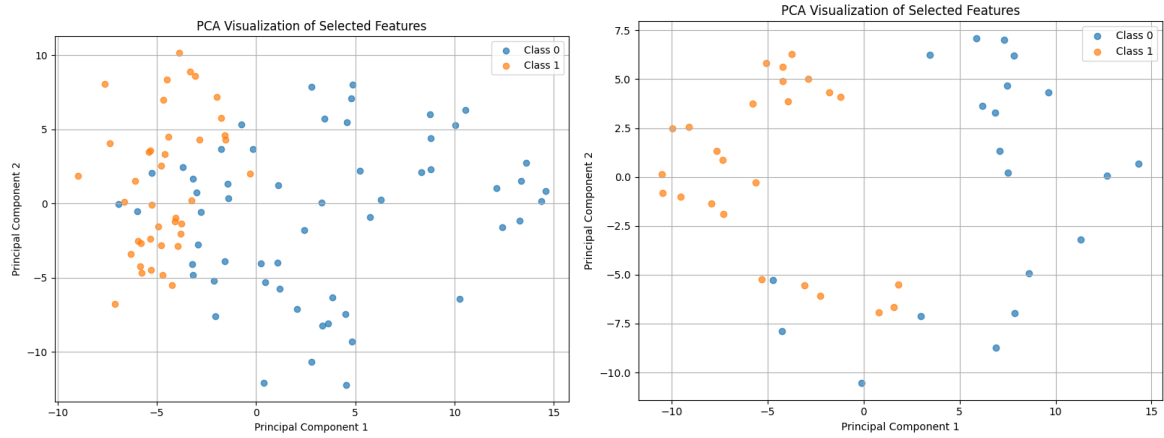


Figure 8. PCA visualization of GA-selected features:(a) MSID dataset (b) MSLD dataset

3.5. Confusion Matrix

Confusion matrices were created for the MSID and MSLD datasets to assess the suggested hybrid framework's classification performance in more detail. These matrices provide light on the different kinds of classification errors, particularly false positives, and false negatives, which are crucial for making clinical decisions. Confusion matrices of MSID Dataset and MSLD Dataset are shown in Figure 9 (a) and Figure 9 (b) respectively.

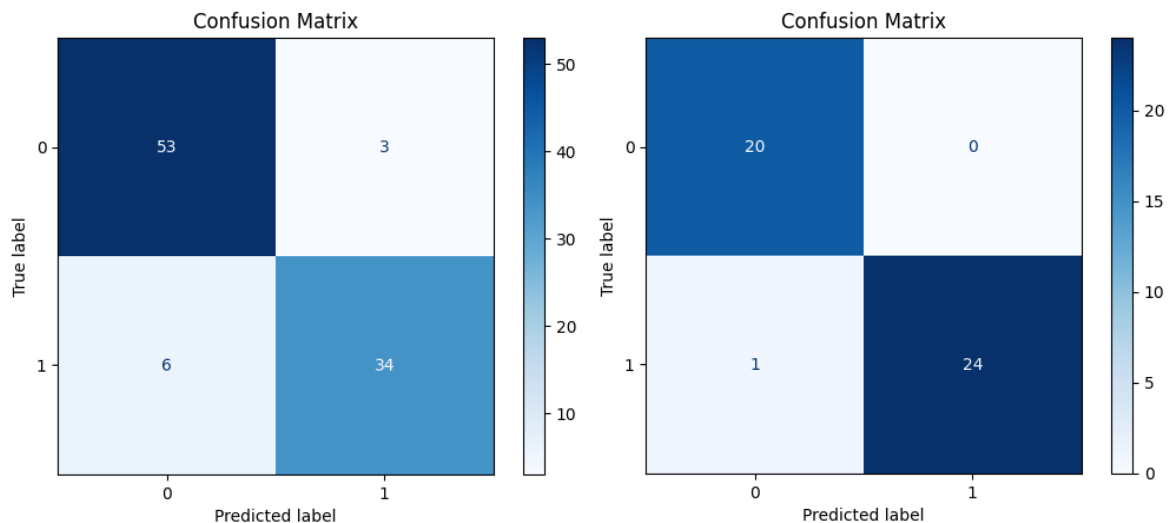


Figure 9. Confusion Matrices (a) MSID (b) MSLD

3.6. Comparative analysis

These findings support the benefits of combining evolutionary optimization, multi-CNN feature fusion, and ensemble learning, particularly in low-resource medical contexts where explainability, speed, and generalization are crucial.

Table 5. Comparative Analysis of previous studies with our work.

Study	Feature Extraction	Feature Selection	Classifier	Accuracy	Key Limitation
Almars (2025) [2]	Attention-based CNN	GA (hyperparameters)	DL head	~90%	No multi-model fusion
Özaltın et al. (2023) [3]	MobileNetV2	None	Softmax	87–90%	No optimization, limited robustness
Shateri et al. (2025) [6]	Xception + NGBoost	AVA Optimization	NGBoost	~94%	No GA-based feature reduction
Alarfaj et al. (2024) [8]	Vision Transformer	None	Softmax	~92%	Computational cost, no ensemble learning
Ours	DenseNet121 +MobileNet	GA	Random Forest	92.71–97.77%	The model has not yet been tested in federated environments.

3.7. Comparative Evaluation of Metaheuristic Algorithms

To evaluate the effects of various optimization methods, 4 metaheuristic algorithms Genetic Algorithm (GA), Whale Optimization Algorithm (WOA), Grey Wolf Optimization (GWO), and Artificial Bee Colony (ABC) were combined in DenseNet121 + MobileNetV2 feature-fusion architecture to classify the Monkeypox disease and the findings are presented in Table 6. The overall performance of GA was the highest and led to the highest accuracy and smallest reduction of features. GA is an excellent recombiner of useful substructures, i.e. cluster of features. This has a direct positive effect on accuracy in classification.

Table 6. Comparison of GA, GWO, WOA, and ABC for Monkeypox detection

Metaheuristics algorithms	Metrics	MSLD	MSID
WOA	Precision	91.00	94.00
	Recall	84.00	85.00
	F1-Score	88.00	89.00
	Test Accuracy (%)	86.67	90.62
ABC	Precision	95.83	87.8
	Recall	92.00	90.00
	F1-Score	93.88	88.89
	Test Accuracy (%)	93.33	90.62
GWO	Precision	95.56	88.37
	Recall	95.56	95.00
	F1-Score	95.56	91.57
	Test Accuracy (%)	95.56	92.71
GA	Precision	100.00	90.24
	Recall	96.00	92.50
	F1-Score	98.00	91.36

	Test Accuracy (%)	97.77	92.71
--	-------------------	-------	-------

Figure 10 represents the comparison of various metaheuristic algorithms with GA used in our framework. The comparative analysis demonstrates that the Genetic Algorithm (GA) achieved the best overall performance within the proposed DenseNet121 + MobileNetV2 hybrid feature-fusion framework. These findings indicate that GA's crossover–mutation dynamics are highly effective for selecting discriminative deep features, leading to robust generalization and superior classification performance.

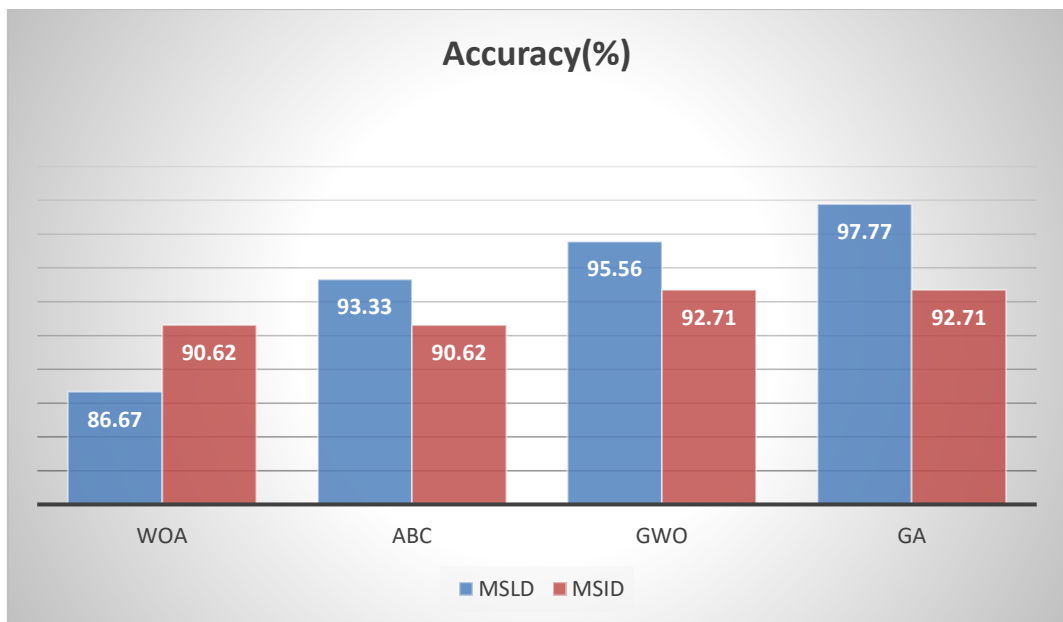


Figure 10. Accuracies bar chart comparison of our framework

3.8. Interpretation and Limitations

Interpretation of Results:

These high classification accuracies of the proposed framework can be explained by the synergistic combination of the framework elements: Dual CNN Feature Fusion: DenseNet121 and MobileNetV2 are used together to provide more and different feature representation, as both fine-grained and high-level features are captured. This increases the discriminative ability of input space. Genetic Algorithm of Feature Selection: GA is a very useful technique to minimize the dimension of features that only contain valuable information. This does not only enhance the performance of the classification but also prevents overfitting and less computation. Random Forest Classifier: RF has great generalization power, noise resistant behavior, and can perform a built-in analysis of feature importance. These attributes render it suitable to the high-dimensional and moderately imbalanced medical image datasets. Cross-Dataset Consistency: The framework recorded good scores on MSID and MSLD, which highlights its generalizability and strength to different datasets structures and class distribution.

Limitations:

Although these positive outcomes have been achieved, one should admit several limitations:

- Dataset Size: MSID and MSLD also have rather small and slightly uneven test sets. Although augmentation and cross-validation are useful, to deploy in the real world, validation on more large and varied datasets is needed.
- Focus of Binary Classification: This paper deals with a binary classification problem (Monkeypox vs. Normal). Nonetheless, practical skin lesion classification can be associated with several

disease categories (e.g., chickenpox, measles, eczema), and it must be extended to multi-class models in the future.

4. Conclusion

This paper introduces a new model of hybrid diagnosis of automated Monkeypox detection by skin lesion images, combining deep learning, evolutionary optimization, and ensemble classification advantages. The method is a combination of the DenseNet121 and MobileNetV2-based dual-feature extraction, Genetic Algorithm-based feature selection, and final prediction with the help of a random forest classifier. Genetic Algorithm was much better since it reduced redundant features, but the strength of the Random Forest was that it was robust, easy to interpret, and highly generalized to the data. Although the results are promising, there are still some limitations, including the size of the dataset, binary classification, and the cost of computation. The future work will focus on exploring federated learning or privacy-friendly modifications of secure clinical applications. Altogether, the contributions of this work provide a strong and practical diagnostic model that connects the world of deep learning with the classical machine learning and provides a scalable solution to AI-aided Monkeypox detection in various health settings.

References

- [1] Su, G., Li, H., Chen, H. (2025). ParMamba: A Parallel Architecture Using CNN and Mamba for Brain Tumor Classification. *Computer Modeling in Engineering & Sciences*, 142(3), 2527–2545. <https://doi.org/10.32604/cmes.2025.059452>
- [2] Nayak, T., Chadaga, K., Sampathila, N., Mayrose, H., Gokulkrishnan, N., Bairy, G. M., Prabhu, S., & Umakanth, S. (2023). Deep learning-based detection of Monkeypox virus using skin lesion images. *Medicine in Novel Technology and Devices*, 18, 100243. <https://doi.org/10.1016/j.medntd.2023.100243>
- [3] Almars, A. M. (2025). DeepGenMon: A novel framework for Monkeypox classification integrating lightweight attention-based deep learning and a genetic algorithm. *Diagnostics*, 15(2), 130. <https://doi.org/10.3390/diagnostics15020130>
- [4] Özaltn, Ö., & Yeniay, Ö. (2023). Detection of Monkeypox disease from skin lesion images using MobileNetV2 architecture. *Communications Faculty of Sciences University of Ankara Series A1: Mathematics and Statistics*, 72, 482–499. <https://doi.org/10.31801/cfsuasmas.1202806>
- [5] Javed, R., Rahim, M. S. M., Saba, T., et al. (2020). A comparative study of features selection for skin lesion detection from dermoscopic images. *Network Modeling Analysis in Health Informatics and Bioinformatics*, 9, 4. <https://doi.org/10.1007/s13721-019-0209-1>
- [6] Khan, M. A., Muhammad, K., Sharif, M., Akram, T., & de Albuquerque, V. H. C. (2021). Multi-class skin lesion detection and classification via teledermatology. *IEEE Journal of Biomedical and Health Informatics*, 25(12), 4267–4275. <https://doi.org/10.1109/JBHI.2021.3070499>
- [7] Eliwa, E.H.I., El Koshiry, A.M., Abd El-Hafeez, T. et al. Utilizing convolutional neural networks to classify monkeypox skin lesions. *Sci Rep* 13, 14495 (2023). <https://doi.org/10.1038/s41598-023-41545-z>
- [8] Latha, D. M., Anusha, K., Samrin, R., Reddy, P. C. S., Sudhakar, B., & Sathish, G. (2024). Classification of skin diseases in the Internet of Medical Things using hybrid deep learning. In *2024 Second International Conference on Networks, Multimedia and Information Technology (NMITCON)* (pp. 1–7). IEEE. <https://doi.org/10.1109/NMITCON62075.2024.10699084>

[9] Alarfaj, A. A., Ahmad, S., Hakeem, A. M., et al. (2024). Novel vision transformer and data augmentation technique for efficient detection of Monkeypox disease. *Multimedia Tools and Applications*. <https://doi.org/10.1007/s11042-024-20456-9>

[10] Vandana, Sharma, A., Chahal, A., & Daryal, N. (2024). Efficient Monkeypox detection in skin lesions using pre-trained deep learning technique. In *2024 International Conference on Artificial Intelligence and Quantum Computation-Based Sensor Application (ICAIQSA)* (pp. 1–7). IEEE. <https://doi.org/10.1109/ICAIQSA64000.2024.10882406>

[11] Desai, P., Barve, A., & Shkokar, K. (2025). A systematic review on Monkeypox skin disease identification approaches. In *2025 International Conference on Machine Learning and Autonomous Systems (ICMLAS)* (pp. 602–607). IEEE. <https://doi.org/10.1109/ICMLAS64557.2025.10968867>

[12] Nazeeruddin, E., Latif, G., & Mohammad, N. (2025). Monkeypox and chickenpox skin lesions classification using hybrid deep learning features. In *2025 International Conference on Inventive Computation Technologies (ICICT)* (pp. 1005–1010). IEEE. <https://doi.org/10.1109/ICICT64420.2025.11004913>

[13] Alharbi, A. H., Towfek, S. K., Abdelhamid, A. A., et al. (2023). Diagnosis of Monkeypox disease using transfer learning and binary advanced dipper throated optimization algorithm. *Biomimetics*, 8(3), 313. <https://doi.org/10.3390/biomimetics8030313>

[14] Pal, R., et al. (2023). Deep and transfer learning approaches for automated early detection of Monkeypox alongside other similar skin lesions and their classification. *ACS Omega*, 8, 31747–31757. <https://doi.org/10.1021/acsomega.3c02784>

[15] Ciran, A., & Özbay, E. (2023). Optimization-based feature selection in deep learning methods for Monkeypox skin lesion detection. In *2023 7th International Symposium on Multidisciplinary Studies and Innovative Technologies (ISMSIT)* (pp. 1–6). IEEE. <https://doi.org/10.1109/ISMSIT58785.2023.10304930>

[16] Uysal, F. (2023). Detection of Monkeypox disease from human skin images with a hybrid deep learning model. *Diagnostics*, 13(10), 1772. <https://doi.org/10.3390/diagnostics13101772>

[17] Park, J. B., Na, J. Y., Kim, S. H., et al. (2025). Machine learning assisted noncontact neonatal anthropometry using FMCW radar. *Scientific Reports*, 15, 16125. <https://doi.org/10.1038/s41598-025-99104-7>

[18] Bansal, S., Tripathi, A., Srivastava, S., & Vuppuluri, P. P. (Eds.). (2025). *Nature-inspired Metaheuristic Algorithms: Solving Real World Engineering Problems*. CRC Press. <https://doi.org/10.1201/9781003612858>

[19] Wu, G., Wang, H., Lin, W. et al. FS-DBoost: cross-server energy efficiency and performance prediction in cloud based on transfer regression. *Cluster Comput* 27, 7705–7719 (2024). <https://doi.org/10.1007/s10586-024-04370-1>

[20] Vommi, V., Kasarapu, R.V. Economic design of control charts considering process shift distributions. *J Ind Eng Int* 10, 163–171 (2014). <https://doi.org/10.1007/s40092-014-0086-2>

[21] Çetintas, D. (2025). Efficient Monkeypox detection using hybrid lightweight CNN architectures and optimized SVM with grid search on imbalanced data. *Signal, Image and Video Processing*, 19, 336. <https://doi.org/10.1007/s11760-025-03915-0>

[22] Alharthi, N. M., & Alzahrani, S. M. (2023). Vision Transformers and Transfer Learning Approaches for Arabic Sign Language Recognition. *Applied Sciences*, 13(21), 11625. <https://doi.org/10.3390/app132111625>

[23] Amna Bamaqa, Waleed M. Bahgat, Yousry AbdulAzeem, Hossam Magdy Balaha, Mahmoud Badawy, Mostafa A. Elhosseini, Early detection of monkeypox: Analysis and optimization of pretrained deep learning models using the Sparrow Search Algorithm, *Results in Engineering*, Volume 24, 2024, 102985, ISSN 2590-1230, <https://doi.org/10.1016/j.rineng.2024.102985>.

[24] Gupta, A., Bhagat, M. & Jain, V. Blockchain-enabled healthcare monitoring system for early Monkeypox detection. *J Supercomput* **79**, 15675–15699 (2023). <https://doi.org/10.1007/s11227-023-05288-y>

[25] Wu, G., Wang, H., Lin, W. *et al.* FS-DBoost: cross-server energy efficiency and performance prediction in cloud based on transfer regression. *Cluster Comput* **27**, 7705–7719 (2024). <https://doi.org/10.1007/s10586-024-04370-1>

[26] J. Zhou, M. Khushi, M. A. Moni, S. Uddin and S. K. Poon, "Lung Cancer Prediction Using Curriculum Learning Based Deep Neural Networks," *2021 IEEE International Conference on Digital Health (ICDH)*, Chicago, IL, USA, 2021, pp. 11-18, doi: 10.1109/ICDH52753.2021.00013.

[27] Sharma, J., Al-Huqail, A.A., Almogren, A. *et al.* Deep learning based ensemble model for accurate tomato leaf disease classification by leveraging ResNet50 and MobileNetV2 architectures. *Sci Rep* **15**, 13904 (2025). <https://doi.org/10.1038/s41598-025-98015-x>

[28] Taha, R., Zain El Abdin, H., & Musleh, T. (2025). Comparative analysis of supervised machine learning models for PCOS prediction using clinical data. *Journal of Engineering Research and Sciences*, 4(6), 16–26. <https://doi.org/10.55708/jsr0406003>